Int. J. Multiphase Flow Vol. 13, No. 5, pp. 685–698, 1987
Printed in Great Britain.

0301-9322/87 $3.00 + 0.00

A METHOD TO MEASURE MASS AND VOLUME FLOW RATES OF TWO-PHASE FLOWS

J. DOMNICK, F. DURST, H. RASZILLIER and H. ZEISEL
LSTM-Erlangen, Lehrstuhl für Strömungsmechanik, Universität Erlangen-Nürnberg, Egerlandstraße 13, 8520 Erlangen, B.R.D.

(*Received* 24 *May* 1985; *in revised form* 8 *March* 1987)

Abstract—The present paper describes a method to measure simultaneously the individual mass and volume flow rates of a particulate two-phase fluid flowing through ducts. A mass flow meter, based on Coriolis force measurements, and an inductive volume flow rate meter were employed in sequence and measured the total (volume and mass) flow rates $\dot{V}_{tot}$ and $\dot{m}_{tot}$ of a fluid–solid two-phase flow. The individual volume and mass flow rates were computed from them and from the known densities of the components. Arguments are presented for and experimental information is given to support the fact that the Coriolis flow meter is able to measure the total mass flow rate of a particulate two-phase flow, if one takes care that the particles in the flow follow the oscillations of the measuring instrument (and the fluid). The inductive volume flow rate instrument is argued to give in a particulate flow, under conditions of homogeneity and suitable limitations on the mean relative velocity between the phases, a good measurement of the total volume flow rate. This is confirmed experimentally in a water flow loaded with sand. It is shown that the possible (relative) error of the volume flow rate in such a flow is bounded by the relative velocity; in the natural flow limits of the water–sand system this error turns out to be one order of magnitude smaller than the relative velocity. The relative velocity can be estimated and the level of accuracy required for the measurements then determines the lower limit of the range of flow rates accessible within it. Accuracy considerations are presented in the appendix.

1. INTRODUCTION

Two-phase flows play an important role in many fields of engineering and a large number of papers exist which deal with such flows and their measurement (e.g. Banerjee & Lahey 1981; John & Reimann 1984). To obtain mass flow rates, particular attempts have been undertaken in chemical process engineering where two-phase flow transport is used to bring reacting components jointly into a reactor vessel where controlled chemical processes take place. Of course, this control requires detailed knowledge of the individual mass flow rates of the reactants supplied to the vessel and, hence, detailed measurement of both mass flows of a two-phase fluid. This information is presently difficult to obtain if the two reactants are made up of different phases, e.g. a gas and a solid, a liquid and a solid or a liquid and a gas. It is very obvious that there is a need in industry to have measuring systems available that are able to measure separately in two-phase flows individual mass or volume flow rates.

The need for measuring both mass flow rates (or volume flow rates) of a two-phase flow mixture is also apparent if one considers the measuring problems present in the pneumatic and hydraulic transport of materials. In the field of civil engineering, sand dredging is a problem that might be mentioned in this respect. A measuring system that is able to record both the water flow and the supplied sand to the dredging pipe system would be a very valuable instrument for answering questions relating to the payment of the supplied sand. There is definitely a lack of measuring equipment applicable to two-phase flows to yield simultaneous information on the mass or volume flow rates of both phases.

Most of the existing instruments to measure mass or volume flow rates are developed for single-phase flow systems and in many applications to two-phase flows it has been assumed that the application of these instruments in two-phase flows is feasible by a calibration of the instrument for a special flow system and particular mixture of the two phases. However, it is well-known that a variation of the mixture of the two phases will result in a change in measured information that cannot be distinguished from changes in the total mass or volume flow rate. Hence, measurements become difficult when mass flow rates and mixture ratios of a two-phase flow change.

Due to the fact that most two-phase flow instruments are extensions of measuring principles developed for single-phase flows, a velocity difference between the phases becomes a negative influence in measurements. Therefore, if measuring devices that are insensitive to relative velocity are available, these should be chosen when measuring devices are developed to obtain mass or volume flow rate information in two-phase flows. If measuring systems insensitive to relative velocity are not readily available, the influence of relative velocity has to be asserted and taken into account when two-phase flow measurements are evaluated.

In many laboratory applications, accurate measurements of the mass flow rates of the two phases are obtained in a discontinuous way by sampling the two-phase flow mixture for a measured or known time increment and by weighing the collected mass of both phases and of one of the phases after separation. This is too complicated a method for many applications, and because of this, instruments have been developed which are capable of making continuous measurements. These instruments have mainly found their application in the field of nuclear reactor technology and are particularly useful in gas–liquid two-phase flows. A summary of existing instrumentation in this field of research is given by Reimann *et al.* (1982). It has to be pointed out that almost all these instruments measure the mass or volume flow rate indirectly, e.g. by recording its influence on the temperature of a sensor, the drag of a plate, the pressure drop across an orifice etc. When, in addition, some information on the mixture composition is obtained the individual mass flow rates can be computed, if the composition and the measured quantity is in the range the instrument has been calibrated for.

In the present paper, another method for obtaining the individual mass or volume flow rates of a two-phase flow is presented. It is based on two flow meters, namely on a Coriolis force meter and an inductive volume rate meter which measure the total mass and total volume rates of the two-phase flow. Knowing both the total mass flow rate and the total volume rate allows the individual flow or mass flow rates to be computed. This is explained in the paper and results of verification experiments demonstrate the functioning of the combined instrument.

Section 2 presents a summary of the measuring principles employed in Coriolis force mass flow meters and inductive volume flow meters with particular attention being given to their application in two-phase flows. For the measuring system proposed by the authors, information on the measurement principles is provided and the basic equations used to evaluate the individual mass or volume flow rates are given in section 3. The employed test loop for verification experiments is described in section 4 and some of the results obtained using this test loop and the proposed measuring, device are given in section 5. Conclusions are provided in section 6 and accuracy considerations are presented in the appendix.

2. EMPLOYED INSTRUMENTS AND APPLICABILITY IN TWO-PHASE FLOWS

The present paper describes the employment of two measuring instruments that have been extensively employed for mass and volume flow rate measurements in single-phase flows:

- Coriolis force mass flow rate meter.
- Inductive volume flow rate meter.

The functioning of both instruments is well-understood when applied to single-phase flow measurements, but questions regarding their correct functioning arise when applications to two-phase flows are considered. Because of this, detailed theoretical studies were carried out and verification experiments performed to determine under what flow conditions and for what kind of two-phase flows the above meters can be employed for accurate measurements. Details of these studies are given by Durst & Raszillier (1986), but a summary of the work is presented below.

2.1. Coriolis Force Mass Flow Rate Meter

This instrument is based on the idea that if a mechanical system is forced to move in a noninertial reference frame, then it experiences force in addition to the ordinary inertial force and the applied (external) physical force. A very simple illustration is provided by a mass point moving on a circle (with constant linear velocity v) which oscillates around an axis parallel to a diameter. It is most convenient to let the axis of oscillation just touch the circle (figure 1). If the oscillation is described

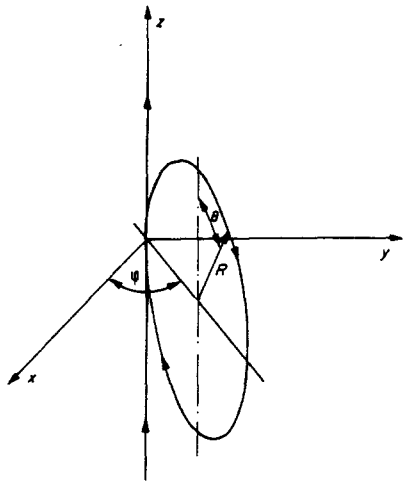

Figure 1. Movement of a continuous mass distribution along an oscillating circle.

by $\varphi(t) = \varphi_0 \sin \omega t$, then the reaction force exerted by the particle perpendicular to the plane of the circle is (in the sense of increasing φ) given by

$$F_\varphi(t) = -2\, mv\omega\varphi_0 \cos \omega t \cdot \cos \theta + mR\varphi_0\omega^2 \sin \omega t \cdot (1 + \sin \theta), \quad \theta = \frac{v}{R} t, \qquad [1]$$

where m is the particle mass. The first term is the Coriolis force $\mathbf{F}_c = +2 \cdot \mathbf{p} \times \boldsymbol{\Omega}$, determined by the particle momentum

$$\mathbf{p} = m\mathbf{v}(|\mathbf{v}| = v)$$

and the angular velocity $\boldsymbol{\Omega}$ of the circle ($|\boldsymbol{\Omega}| = \omega\varphi_0 \cos \omega t$), whereas the second term is an inertial force due to the nonuniform movement of the circle. The part of interest is the Coriolis force because of its proportionality to $|\mathbf{p}| = mv$, the particle momentum. If there are many particles moving with the same velocity, their forces (depending on their positions on the circle) will sum. One may conceive therefore the situation where the whole circle is covered by (a uniform distribution of) particles moving with velocity v, which is a simulation of a fluid flowing with uniform velocity. In this situation one takes, in order to single out the Coriolis forces, their moment with respect to a diameter perpendicular to the oscillation axis; the ordinary inertial component does not contribute to this moment because it acts symmetrically to this axis. The total moment caused by the Coriolis force is given by

$$\mathcal{M}_c(t) = -RL\dot{M}\varphi_0\omega \cos \omega t, \qquad [2]$$

where $L = 2\pi R$ is the length of the oscillating circle and

$$\dot{M} = \rho v = \left(\frac{M}{L}\right) v \qquad [3]$$

is the mass flow rate (M = total mass on the circle, M/L = mass on unit length), which is the central idea on which the Coriolis mass flow rate measuring device is based. One measures the amplitude

$$\mathcal{M}_{c0} = RL\dot{M}\omega\varphi_0 \qquad [4]$$

of the moment $\mathcal{M}_c(t)$ and the oscillation amplitude φ_0, and computes

$$\dot{M} = \mathcal{M}_{c0}(\varphi_0 RL\omega)^{-1} \qquad [5]$$

for known values of the constants R, L, ω.

By imagining several circles oscillating together, but with particle distributions moving with different (masses and) velocities, one notices that the device does measure the mass flow rate $\dot{M}$ for a fluid in a pipe, irrespective of the velocity profile, as long as one may neglect the diameter of the pipe compared to its radius of curvature. The fluid may be imagined to flow along the

oscillation axis, pass through the circular part, and leave it again at the point of contact in order to flow away along the axis.

If the amplitude φ_0 is the response to the excitation by a harmonic force of constant amplitude (and frequency ω), then its magnitude will depend on the proper frequency of the oscillating system, i.e. on the elastic constant and on the oscillating mass (pipe plus fluid). Its measurement gives therefore the fluid mass and (for known volume) its density. In conclusion, by measuring φ_0 one can obtain the fluid density, and through the additional measurement of the moment $\mathcal{M}_c$ one also obtains the mass flow rate of the fluid.

For a two-phase flow nothing new is expected to happen as long as the transverse dimensions of the pipe are negligible, as was considered to be the case for the single phase. In this extremely idealized situation the device has to work as well in two-phase flows as it does for one-phase flows. If these dimensions start to get nonnegligible, then problems will arise. Their origin lies in the fact that when a pipe oscillates, an incompressible fluid has to oscillate with it, but small (solid) particles are forced to do so only inasmuch as the drag force or their collision with the pipe wall achieve this. Drag forces (say according to the Stokes law) are big if the dimensionless parameter

$$u = \omega \frac{m_p}{6\pi\mu R_p} = \frac{4 R_p^2 \rho_p}{18 \mu} \omega \qquad [6]$$

is < 1 (ρ_p = density of the particle substance, R_p = particle radius, μ = dynamic viscosity). If there are no wall effects, for high values of u (big particles, small viscosity or high frequency) the particles will follow the fluid with more and more difficulty. As a consequence, the oscillating mass becomes systematically smaller than the physical mass in the oscillating pipe. This leads to a systematic underestimation of the density of the fluid mixture.

One has to consider also the effect of the magnitude of the pipe diameter. There are more and more particle–wall collisions when the diameter decreases, as can be shown also by analytic calculations (Durst & Raszillier 1986). These calculations also show that the contribution to the Coriolis force moment coming from the particles increases precisely to

$$-RL\dot{M}_p \varphi_o \omega \cos \omega t \qquad [7]$$

($\dot{M}_p$ = solid-phase mass flow rate) in the extreme cases when either $\mu \to \infty$ (high viscosity) or $d \to 0$ (d = pipe diameter). In the intermediate situations both effects, viscosity and particle–wall collisions contribute to the Coriolis moment, so one expects the formula

$$\mathcal{M}_c(t) = -RL(\dot{M} + \dot{M}_p)\varphi_0 \omega \cos \omega t \qquad [8]$$

to be valid for $u = (4 \rho_p R_p^2 / 18 \mu)\omega$ of the order of unity (and not just for $u < 1$). In this range one expects the Coriolis mass flow rate meter to work well in two-phase (solid and liquid) flow.

The dependence of the amplitude φ_0 of the pipe oscillation on the mass of the solid phase is a more complicated matter, since viscosity and wall collisions may have opposite effects on the proper oscillation frequency of the pipe: higher viscosity ($\mu \to \infty$) decreases the frequency, whereas small diameter ($d \to 0$) increases it. One expects from this a decrease in the sensitivity of the amplitude with respect to the mass of the solid phase, which means a decrease in precision in the density determination from φ_0.

It was mentioned in the introduction of this paper, that two-phase flow instruments to measure the mass or volume flow rates of both phases should employ instruments that are insensitive to relative velocity. The Coriolis force meter is such a device which can readily be deduced from the considerations given above. This is also proved in the experimental part of this paper, see section 5.2.

2.2. Inductive Volume Flow Rate Meter

The principle of this measuring device rests on the (Lorentz) force (**F**), which a charged particle (charge q) perceives when moving in a magnetic field **B** with velocity **v**:

$$\mathbf{F} = q\left(\frac{\mathbf{v}}{c} \times \mathbf{B}\right) \quad (c = \text{speed of light}). \qquad [9]$$

The force acts perpendicularly to the plane determined by the vectors $\mathbf{v}$ and $\mathbf{B}$, in opposite senses for charges of opposite signs. Therefore, if there is a given flow (of a fluid) of positive and negative charges with (say constant) velocity $\mathbf{v}$, with a magnetic field $\mathbf{B}$ applied perpendicular to the flow, the charges will be separated in the direction $\mathbf{n} = \mathbf{v} \times \mathbf{B}/|\mathbf{v} \times \mathbf{B}|$, creating along it an electric field $\mathbf{E}$. The electric force generated by the field $\mathbf{E}$ opposes the magnetic one and, in the equilibrium situation, matches it exactly. In the equilibrium the potential difference U between opposite wall points, created by the electric field, is thus proportional to B and to v (if $\mathbf{v}$ is constant through the flow section): $U = K \cdot v \cdot B$ ($K = \text{const}$). If there is a velocity *distribution* over the flow cross section, then $U = \int \mathbf{E} \cdot \mathbf{n}\, dx$ (x = coordinate in the direction $\mathbf{n}$) is expected to be proportional to $\bar{v}$, the *mean* fluid flow velocity.

The quantitative evaluation of $\mathbf{E}$ is most suitably done over the solution of Maxwell's equations (e.g. Engl 1961), i.e. on the phenomenological level, where the existence of (mobile) electric charges is simulated by the nonvanishing electric conductivity σ. Its magnitude will differ, whether we have a metallic conductor or an electrolytic one, as one may expect to have in the present situation. The field $\mathbf{E}$ will depend on the value of σ, in general, but for high enough values of σ (high charge mobility, many charge carriers) it becomes insensitive to it. The level, at which this happens, includes fluids with small natural electrolytic impurities like (ordinary, not distilled) water.

Considering now two-phase flows, of a (electrolytic) liquid with a solid dielectric (particle) phase mixed into it, one has two effects at the phenomenological level: a decrease of conductivity σ, and (perhaps) a change in the velocity distribution. As long as one remains above the sensitivity level for σ, no significant conductivity effect on U is to be expected. On the other side, all quantitative insight into the potential difference U rests on the assumption of an *electrically homogeneous medium*, i.e. without permitivity and conductivity *gradients* over the flow cross section. An inhomogeneously distributed particle phase will violate this assumption and is expected to lead to a deviation from $U = K \cdot v \cdot B$.

Finally, in a (stationary) flow there may appear a velocity difference between the liquid phase and the dispersed particle phase. This could be the case mainly in vertical flow, which is preferable in measuring devices for reasons of homogeneity. The relative velocity due to gravity is dependent on the particle size. Qualitatively it behaves for small particles like R_p^2 and changes with increasing particle size towards a behavior like $R_p^{1/2}$. Quantitatively the relative velocity may be evaluated by equating the drag and gravity forces acting on a particle. When it turns out to be considerable, then the question as to whether the inductive measuring device gives the mean velocity $\bar{v}_{tot}$ of the two-phase mixture or the mean fluid velocity $\bar{v}_f$ becomes relevant. In the present paper this question is not elaborated upon. Namely, it will be shown (in section 5.2) that the experimental results indicate the absence of relative velocity in the water–solid mixture studies in this paper. The quantitative estimation of the relative velocity confirms the experimental finding. In the situation considered here the inductive flow rate meter therefore gives the total volume flow rate of the two-phase system.

3. MEASURING PRINCIPLE AND REQUIRED INSTRUMENTATION FOR TWO-PHASE FLOW MEASUREMENTS

The aim of the research at LSTM-Erlangen has been to yield a measuring system for the determination of the mass flow rate of each of the phases of a two-phase fluid, especially for particle-loaded liquid flows. The instruments described in section 2 allow the determination of the total mass and volume flow rates of a two-phase flow, i.e. the measurement of $\dot{m}_{tot}$ and $\dot{V}_{tot}$. If these instruments are combined, the two individual mass or volume flow rates of a two-phase fluid can be measured as shown below.

The following equations describe the mass and volume fluxes for a two-phase flow:

$$\dot{m}_i = \rho_i \dot{V}_i, \qquad i = \text{f, p}, \tag{10}$$

$$\dot{V}_{tot} = \dot{V}_f + \dot{V}_p, \quad \dot{m}_{tot} = \dot{m}_f + \dot{m}_p, \tag{11}$$

with the following definitions of the subscripts: f = fluid; p = particle; tot = total two-phase mixture. From [10] and [11] one can obtain simple expressions for the volume flux and the mass flux of the two phases:

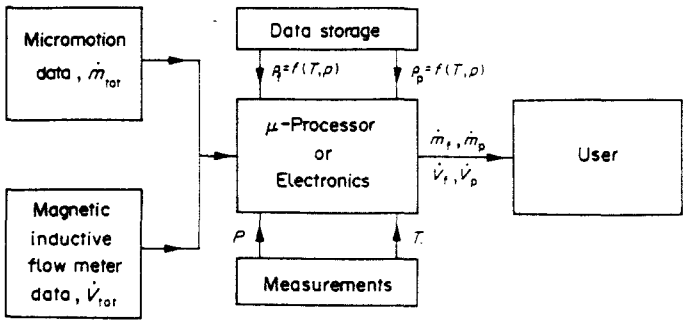

Figure 2. The developed measurement system.

$$\dot{V}_p = \frac{\dot{m}_{tot} - \rho_f \dot{V}_{tot}}{\rho_p - \rho_f}, \qquad \dot{V}_f = \frac{\rho_p \dot{V}_{tot} - \dot{m}_{tot}}{\rho_p - \rho_f}, \tag{12a}$$

$$\dot{m}_p = \rho_p \frac{\dot{m}_{tot} - \rho_f \dot{V}_{tot}}{\rho_p - \rho_f}, \qquad \dot{m}_f = \rho_f \frac{\rho_p \dot{V}_{tot} - \dot{m}_{tot}}{\rho_p - \rho_f}. \tag{12b}$$

If the densities of the two components of the two-phase flow are known, only the total mass flow rate $\dot{m}_{tot}$ and the total volume flow rate $\dot{V}_{tot}$ need be measured in order to find the mass and volume flow rates of each of the phases. Since the density of solid particles in practice does not change with temperature T and pressure P and also the density of the liquid phase does not depend drastically on P and T, the densities of both phases can be taken to be known in all parts of the test section employed in the present study and accurate measurements of both mass or volume flow rates are possible without further information. If the fluid density is pressure and temperature dependent measurements of both T and P are necessary to yield accurate values for the relevant densities of both phases of the fluid. For most common components of two-phase fluid systems, the dependence of the densities on temperature and pressure is known.

For the measurement of the two required quantities $\dot{m}_{tot}$ and $\dot{V}_{tot}$ Micro-Motion Coriolis force meter (MM)† and a magnetic inductive flow meter (MI),‡ respectively, were used. Figure 2 shows a block diagram of a measuring system consisting of the MM and MI instruments. As seen from the diagram , the signals of the MM and MI instruments were fed into a microprocessor, which provides the individual flow rates of the two-phase flow.

4. TEST LOOP AND INSTRUMENTATION

In order to test the measuring system described in section 3, a test facility was built at LSTM-Erlangen which allows for defined particle-loaded flows and for reference measurements of the actual loading of particles in the fluid. The test facility is shown in figure 3. It embraced three major parts: a stirring tank (11), a two-phase fluid pump (1) and the actual test loop consisting of pipe arrangements for the flow. Additional equipment, like pressure sensors, temperature sensors, gravimetric and volumetric instrumentations etc, employed in the tests to obtain well-defined flow conditions so that a direct comparison of known flow properties with measured quantities became possible is not completely shown in figure 3.

The two-phase fluid flow in the test loop was set up by mixing the test liquid (water in the present case) and the employed particles (sand particles) in the stirring tank using a specially designed Intermig®-Impeller. The stirring tank had a capacity of 1.4 m^3 and was built to withstand pressures up to 16 b. On the inside, the stirring tank was coated with an 8 mm rubber layer which guarantees a long lifetime despite the continuous stirring of the particle–fluid mixture. The four stream refractioners in the tank were coated with a rubber layer of 14 mm.

†See *Instruction Manual*: *Micro-Motion*.
‡See *Instruction Manuals*: *Krohne* or *Flowtech*.

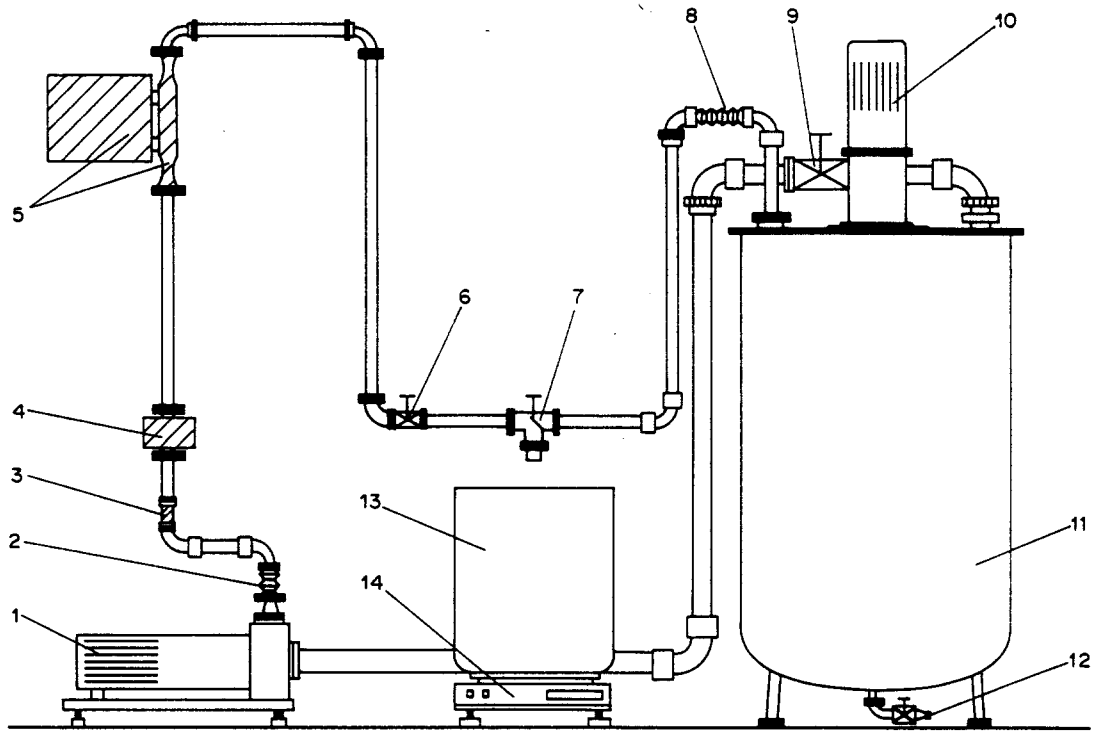

Figure 3. Mechanical components of the test rig: 1, pump; 2, compensator; 3, window; 4, inductive flow meter; 5, Coriolis mass flow rate meter; 6, valve; 7, three-way valve; 8, compensator; 9, valve; 10, stirring motor; 11, two-phase tank; 12, outlet; 13, tank; 14, scale.

After passing through the valve (9) the two-phase flow entered the centrifugal pump (1). This pump was coated with a layer of polyethylene which does not impair the particles and guarantees a long lifetime for the pump. The maximum volume rate of the pump is 20 m^3/h and its total head under standard conditions is about 4 b. After a reduction of the tube diameter from 32 to 25 mm and a vibration compensator (2), introduced to eliminate effects of pump vibrations on the measuring devices, the two-phase flow reached the pipe system of the loop. As figure 3 shows, the pipe arrangement can easily be modified to measure flows in the direction of and against the gravity leaving all other flow conditions equal.

The actual pipe test loop was built of stainless-steel pipes with 25 mm i.d. and was designed to resist maximum pressures of 16 b. A pipe length of 30 diameters was designed to provide a glass section (3), which allowed visual and photometric control of the loading of the flow. Passing this section, the flow reached the electromagnetic (MI) volume flow rate meter (4) and after another length of 30 pipe diameters the Micro-Motion (MM) mass flow rate measuring instrument (5). At the end of the test loop a three-way valve (7) was mounted, which allowed samples of the two-phase test fluid to be taken discontinuously for reference measurements, gravimetric (14) and volumetric (13). In the standard valve position the flow came back to the stirring tank passing a vibration compensator (8) pipe insert. In the sampling position the fluid left the test loop for reference measurements to yield the total mass and volume flow rates, as well as the weight concentration of the two phases.

The running speed of the d.c. motors of the pump and the impeller were continuously controlled by light barriers. Regulation of their speeds to better than 1% over one test run allowed us to maintain constant flow and mixing conditions.

At the beginning and at the end of the test loop, the pressure along the test loop was measured by strain gauge pressure transducers of type P3Ma built by Hottinger–Baldwin–Meßtechnik. The pressure range of these sensors is between 0 and 20 b and their accuracy is better than $\pm 0.2\%$. In addition to pressure measurements, temperature measurements were performed with PT 100 sensors mounted in the stirring tank, in the Micro-Motion flow meter and in the collecting vessel

for the fluid. These sensors have a temperature range of -100 to 199°C with an accuracy of better than $\pm 0.1\%$ of the actual value. All temperature measurements, the pressure information, the information on the revolution of the pump and the impeller etc. were indicated through meter displays mounted at the central switch board of the measuring system. The displayed values were all recorded for further evaluation of the data after the experiments. Data handling was carried out by a Kontron-Ψ-80 microcomputer which also processed the measurements for total mass flow rates $\dot{m}_{tot}$ and the total volume flow rate $\dot{V}_{tot}$.

The gravimetric and volumetric reference data were taken from the test loop under full running conditions: the total weight and volume of samples within given time intervals were measured; from them the loading $x = \dot{m}_p/\dot{m}_{tot}$ of the fluid with particles was derived:

$$x = \frac{\left(1 - \rho_f \frac{\dot{V}_{tot}}{\dot{m}_{tot}}\right)}{\left(1 - \frac{\rho_f}{\rho_p}\right)}. \qquad [13]$$

5. TEST MEASUREMENTS

In order to prepare the test measurements with a two-phase liquid–solid flow, the test loop was filled with water and quartz particles of the size distribution given in figure 4, average dia 0.125 mm, were added. The liquid was continuously stirred, so that the particles remained suspended stationarily in the stirring vessel and a stationary and homogeneous particle-loaded flow was achieved. Rechecking the particle size confirmed that size variations were minimal within the set of experiments.

5.1. Single-phase Flow Measurements

The correct functioning of the employed mass and volume flow rate instruments was assured by comparative measurements in a single-phase (water) flow; results of the comparative tests are shown in figure 5. This figure shows that very close agreement is obtained between the MM and MI measurements over most of the flow range. Only at lower fluid velocities did some differences appear. From comparison with various MI instruments it was concluded that the difference is due to calibration errors of the MI instrument and figure 5 was employed to recalibrate this instrument prior to the measurements in two-phase flows. This was found to be essential for accurate measurements of both components of the mass flow rate especially for low particle concentration and low total flow rates.

5.2. Two-phase Flow Measurements

For the two-phase flow measurement the stirring tank was filled with a known volume of water and sand was added to get a desired mass fraction. Each set of experiments started with a single-phase test to guarantee the correct adjustment of the instruments and then the sand mass fraction was gradually increased.

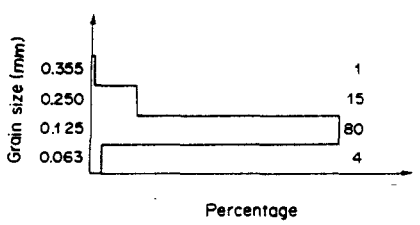

Figure 4. Grain size distribution of the quartz sand used.

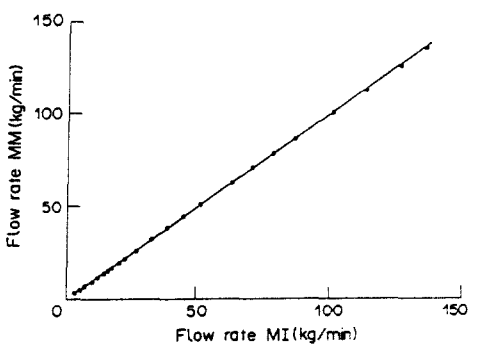

Figure 5. Mass flow rate measured (●) by MM and MI instruments in single-phase flow; test fluid = water.

Table 1

Set No.	Mass fraction (%)	Total mass flux (kg/min)
1	0.5–10.0	20–150
2	2.0–11.5	50–120
3	3.0–22.0	40–100

Altogether three sets of experiments were performed, in the ranges shown in table 1. Each set contains a number of measuring points, each point representing an average value of measurements taken during time intervals varying from 30 s up to several minutes.

The measurements were started by setting the mass fraction of particles and the pump speed. Then the latter was varied in order to see how the volume rate influences the measured values of mass fraction. These values were compared with the reference values of the mass fraction of particles obtained through sampling, as described in section 4, from the reference values of the volume and mass (flow rates) given by a balance and a calibration tank. Figure 6 represents the behaviour of the loadings computed by [13], on the one hand from the flow rate measurement data of the instruments and on the other hand from the reference sampling, as a function of the flow rate. The total mass fraction of sand added to the water in the stirring tank was kept unchanged at about 5%. The values obtained for the loadings are to a high degree independent of the flow rate. There is, in addition, a remarkable agreement between the individual measured and reference values of the loading at various flow rates. In figure 7 the same kind of behaviour is shown to result at a loading of 10%.

For the interpretation of these results it it convenient to consider the reference data separately and from them draw conclusions about the flow. The reference measurements given by their very nature the total flow rates $\dot{m}_{tot}$ and $\dot{V}_{tot}$. If there is a relative velocity between the phases, the ratio $\dot{m}_{tot}/\dot{V}_{tot}$ is velocity (i.e. flow rate) dependent, and thereby also the reference loading x_{ref} given by [13]. The constancy of x_{ref} in figures 6 and 7, therefore, is an indication of the absence of a significant relative velocity.

One may get an idea of the magnitude of the stationary relative velocity by equating the drag and buoyancy forces acting on a particle. The drag force $= \frac{1}{2}\rho_f \pi R_p^2 v_{rel}^2 C_d$, where v_{rel} is the relative velocity and C_d is the drag coefficient, which is well-represented, up to Reynolds numbers $\mathrm{Re} = 2R_p v_{rel}/\nu$ of order 10^5, by the following formula (Brauer 1971, p. 200):

$$C_d = \frac{24}{\mathrm{Re}} + \frac{4}{\mathrm{Re}^{1/2}} + 0.4.$$

The buoyancy force $= \frac{4}{3}\pi R_p^3(\rho_p - \rho_f)g$. For the data of the present experiment ($\rho_p = 2.64 \cdot 10^3\ \mathrm{kg/m^3}$, $\rho_f = 10^3\ \mathrm{kg/m^3}$, $\nu = 10^{-6}\ \mathrm{m^2/s}$, $g = 9.806\ \mathrm{m/s^2}$, $R_p = 1.25 \cdot 10^{-4}\ \mathrm{m}$), the equality

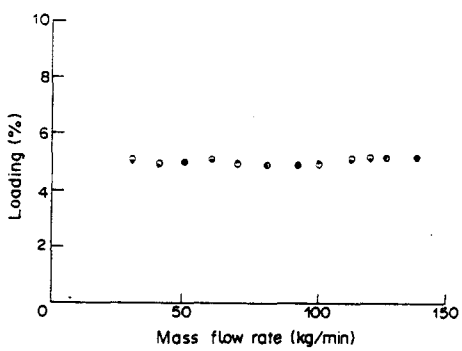

Figure 6. Loading at different mass flow rates at $x = 5.03\%$; comparison between measured loadings (●) and reference values (○).

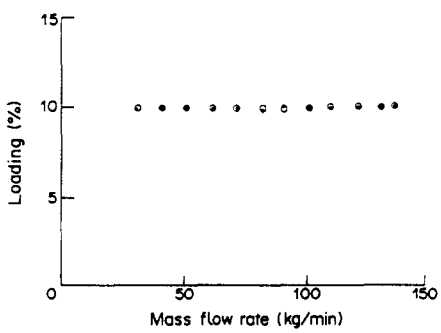

Figure 7. Loading at different mass flow rates at $x = 10\%$; comparison between measured loadings (●) and reference values (○).

$$\tfrac{4}{3}\pi R_p^3(\rho_p - \rho_f)g = \tfrac{1}{2}\pi R_p^2 \rho_f v_{rel}^2 C_d$$

may be transformed into an equation,

$$\mathrm{Re} + \tfrac{1}{6}\mathrm{Re}^{1.2} + \tfrac{1}{60}\mathrm{Re}^2 = 1.745,$$

for the Reynolds number Re, with the (positive) solution Re = 1.427. This number is about 80% of the result (1.745) given by the Stokes drag law. The relative velocity v_{rel} resulting from it is $v_{rel} = 1.142 \cdot 10^{-2}$ m/s. At a volume flow rate of $\dot{V}_{tot} = 10^2$ l/min and a pipe diameter $d = 2.5 \cdot 10^{-2}$ m one has a mean flow velocity $\bar{v}_{tot} = 3.395$ m/s and a ratio $v_{rel}/\bar{v}_{tot} = 0.336 \cdot 10^{-2}$, i.e. 0.336%. At a lower flow rate, of 30 l/min say, the velocity ratio $v_{rel}/\bar{v}_{tot}$ would increase to about 1%.

It is appropriate to add here an estimation of the effect of relative velocity on the deviation of the mean velocity $\bar{v}_{tot} = c_f\bar{v}_f + c_p\bar{v}_p$ (c_f, c_p = volume concentration of the fluid and particle phases, respectively, $c_f + c_p = 1$) from the mean fluid velocity $\bar{v}_f$: $\bar{v}_{tot} - \bar{v}_f = (c_f - 1)\bar{v}_f + c_p\bar{v}_p = c_p(\bar{v}_p - \bar{v}_f) = c_p \cdot v_{rel}$. The relative deviation is thus $(\bar{v}_{tot} - \bar{v}_f)/\bar{v}_{tot} = c_p \cdot v_{rel}/\bar{v}_{tot}$, where the volume concentration c_p is of the order $x \cdot \rho_f/\rho_p \approx 0.38\,x$. For a loading $x < 0.25$ this leads to $c_p < 0.1$. The relative difference between the total mean velocity $\bar{v}_{tot}$ and the mean fluid velocity $\bar{v}_f$ is, as a consequence, an order of magnitude smaller than the relative velocity $v_{rel}/\bar{v}_{tot}$: at a flow rate of 30 l/min, the lower end of the present measurement range, it is about 0.1%, and it decreases even more towards higher flow rates. This explains the extremely good agreement between measurement and reference points in figures 6 and 7 as being independent of whether the inductive flow meter indicates $\bar{v}_{tot}$ or $\bar{v}_f$. It should be noted, that the sign of the relative velocity changes from a flow against gravity to one with it. By comparison of the two flow regimes, which has been especially allowed for in the design of the test loop (section 4), there appears to be a doubling of relative velocity effects. Even so, no relative velocity effect could be detected in the measurements.

The comparison of the measured and reference (volume and mass) flow rates is shown in figures 8 and 9, respectively. The data come from three sets of measurements, covering a wide range of loadings (3.0–22.0%). The agreement between the two (measurement and reference) sets of data turns out to be better than 1%.

Finally, in figure 10 all the measurements of the loading x are represented vs the reference values x_{ref}; the points correspond to (mass) flow rates between 20 and 150 kg/min (table 1). There is excellent agreement between x and x_{ref} in the loading range $x < 0.10$. In the upper part, $0.10 < x < 0.22$, there appears to be an increased scattering of the points around the line $x = x_{ref}$. This scattering has to be ascribed in part to the fact that the errors of the reference (sampling) measurements became nonnegligible compared to those of the instruments, but mainly to a change in the flow regime in the test loop. In this range of rather high loadings phenomena of nonstationarity are expected to be generated in the stirring vessel, as well as in the horizontal parts of the test loop due to onsets of sedimentation. This kind of phenomena have still to be investigated in detail in order to improve the precision of the procedure up to the natural limit of its applicability (around $x \approx 0.25$).

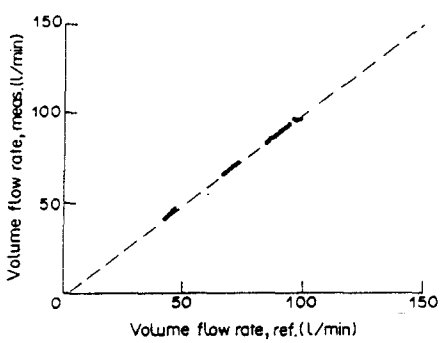

Figure 8. Measured volume flow rate (MI) vs reference volume flow rate for different loadings (3–22%).

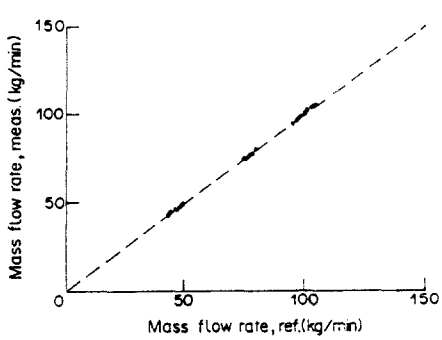

Figure 9. Measured mass flow rate (MM) vs reference mass flow rate for different loadings (3–22%).

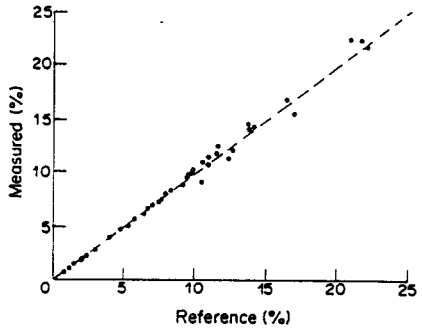

Figure 10. Measured loading vs reference loading for different mass fluxes.

6. CONCLUSIONS

The paper describes measurements of the (volume and mass) flow rates of the individual phases of two-phase fluids (consisting of water and sand particles) flowing in ducts. A system consisting of a Coriolis force mass flow meter and a magnetic inductive volume flow rate meter has been used in order to measure the total volume and mass flow rates, $\dot{V}_{tot}$ and $\dot{m}_{tot}$, respectively, of the mixture. The flow rates of the individual phases are derived from them by computation, assuming the densities of the two phases as given.

Care has to be taken that the flow is homogeneous and the time variations of the flow are small during individual measurements. The results turn out to be rather excellent for a loading below $x \approx 0.1$ and for relative velocities so small that they have no effect on the volume rate $\dot{V}_{tot}$. The relative error of $\dot{V}_{tot}$ from the relative velocity can be bounded by

$$\frac{\Delta \dot{V}_{tot}}{\dot{V}_{tot}} < x \cdot \frac{\rho_f}{\rho_p} \cdot \frac{v_{rel}}{\bar{v}_{tot}};$$

for the present phases it turned out to be typically by one order of magnitude smaller than the relative velocity $v_{rel}/\bar{v}_{tot}$. The relative velocity v_{rel} in turn can be evaluated from the densities, the fluid viscosity and the particle size. In the present case it turned out to be about $v_{rel} \sim 10^{-2}$ m/s. On the lower limit of the flow rate range ($\bar{v}_{tot} = 20$ l/min) this gives $v_{rel}/\bar{v}_{tot} = 1.68 \cdot 10^{-2}$ (i.e. 1.7%) and thereby a negligible possible error $\Delta \dot{V}_{tot}/\dot{V}_{tot} < 1.68 \cdot 10^{-3}$ in the flow rates.

For higher loadings the results remain satisfactory for many practical needs. An increase in accuracy up to the flow limit of the mixture requires, without doubt, a rather deep understanding of the altered flow characteristics of the mixture in this loading range.

Developmental work is being continued in order to automate the measurements and to design an instrument with the evaluation operations being carried out by hardware electronics instead of a microcomputer, as at present. Further work is also being done in order to apply the developed instrument to other two-phase flows, e.g. bubbly liquid flows and gas–liquid flows (sprays), in order to see how the instrument performs under such flow conditions.

Acknowledgement—The authors gratefully acknowledge financial support of this work through the Deutsche Forschungsgemeinschaft, obtained within the Teilprojekt A4 of the Sonderforschungsbereich 222 at the University of Erlangen-Nürnberg.

REFERENCES

BANERJEE, S. & LAHEY, R. T. JR 1981 Advances in two-phase flow instrumentation. *Adv. nucl. Sci. Technol.* **13**, 227–414.

BRAUER, H. 1971 *Grundlagen der Einphasen- und Mehrphasenströmungen.* Sauerländer, Aarau.

DURST, F. & RASZILLIER, H. 1986 Inductive and Coriolis force flow meters and their employment in two-phase flows. To be published.

ENGL, W. 1961 Relativistische Theorie des induktiven Durchflußmessers. *Arch. Elektrotech.* **46**, 173–189.

JOHN, H. & REIMANN, J. 1984 Untersuchung von Instrumentierungen für Zweiphasenströmungen. Report KfK 3630.

REIMANN, J., JOHN, H. & MÜLLER, U. 1982 Measurements of two-phase mass flow rate: a comparison of different techniques. *Int. J. Multiphase Flow* **4**, 141–155.

APPENDIX

Accuracy Considerations

In this appendix we put together some considerations regarding the connection between the accuracy of the loading and that of the total flow rates $\dot{m}_{tot}$ and V_{tot}. It has to be borne in mind that to the error of x, appearing as a propagation of the errors of $\dot{m}_{tot}$ and V_{tot}, one has to add, eventually, errors originating in the limits of validity of the formulae expressing x as a function of $\dot{m}_{tot}$ and $\dot{V}_{tot}$.

The solid mass fraction (loading) of a two-phase flow has been defined by

$$x = \frac{\dot{m}_p}{\dot{m}_{tot}} \qquad [A.1]$$

and can be expressed by [12b] as

$$x = \frac{\left(1 - \rho_f \frac{\dot{V}_{tot}}{\dot{m}_{tot}}\right)}{\left(1 - \frac{\rho_f}{\rho_p}\right)}. \qquad [A.2]$$

The ratio $\dot{m}_{tot}/\dot{V}_{tot}$ is, in fact, a density and consequently one may denote it by ρ_{tot}:

$$\rho_{tot} = \frac{\dot{m}_{tot}}{\dot{V}_{tot}}. \qquad [A.3]$$

The determination of the loading x, as described in section 3, is therefore the result of a density measurement. It is convenient, for the sake of the discussion, to consider the relative densities

$$r_{tot} = \frac{\rho_{tot}}{\rho_f} \quad \text{and} \quad r_p = \frac{\rho_p}{\rho_f}, \qquad [A.4]$$

with respect to the fluid, in order to get

$$x = \frac{\left(1 - \frac{1}{r_{tot}}\right)}{\left(1 - \frac{1}{r_p}\right)} = \frac{r_p}{r_p - 1} \cdot \frac{r_{tot} - 1}{r_{tot}}. \qquad [A.5]$$

One may assume that the error dx in the determination of x appears essentially as the propagation of the error dr_{tot} in the measurement of the density ratio r_{tot}. This yields

$$dx = \frac{r_p}{r_p - 1} \cdot \frac{dr_{tot}}{r_{tot}^2}. \qquad [A.6]$$

Since the present considerations concern situations where $r_p > 1$, we notice that for $r_p \geqslant 2$ one gets an error smaller than $2(dr_{tot}/r_{tot}^2)$, which in turn is smaller than $2\,dr_{tot}$. Thus, the absolute error of the loading in this range is smaller than twice the error of r_{tot}. For very large particle densities, the ratio $(r_p - 1)/r_p \to 1$ and the error of the computed loading approaches the error of the measured density.

In order to get a quantitative picture one may look more closely at the error dx and its dependence on the loading x, for fixed values of the relative error $dz = dr_{tot}/r_{tot}$ of the density ratio r_{tot}. This dependence is linear:

$$dx + x\,dz = \frac{r_p}{r_p - 1} \cdot dz; \qquad [A.7]$$

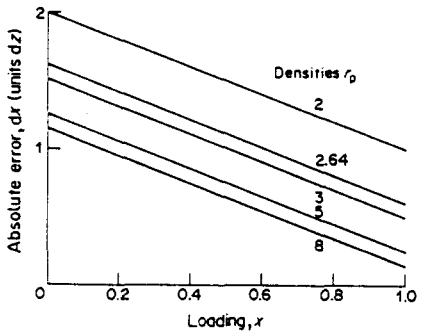

Figure A1. Absolute error dx of loading (in units of dz, the relative error of the density), as a function of loading x, for various particle densities r_p.

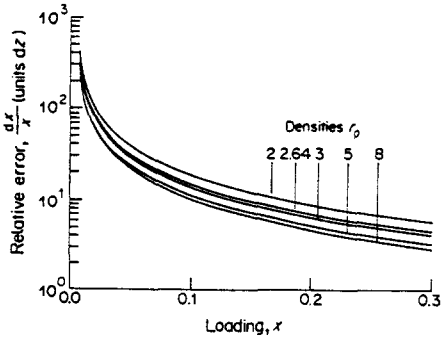

Figure A2. Relative error dx/x of loading (in units of dz), as a function of loading x, for various particle densities r_p.

it interpolates between $dx = dz(r_p/r_p - 1)$ at zero loading $x = 0$ (pure fluid phase) and $dx = dz(1/r_p - 1)$ at the (hypothetical) loading $x = 1$ (pure solid phase).

The lines [A.7] give the lower limits on the loadings down to which one can (theoretically) measure, if the (absolute) error is to be kept within prescribed limits. In figure A1 these lines are presented for various particle densities.

The picture changes dramatically if one is interested in the relative error of loading, dx/x (figure A2). Then, instead of the straight lines [A.7], one gets the hyperbolae

$$\frac{dx}{x} = dz\left(\frac{r_p}{r_p - 1}\cdot\frac{1}{x} - 1\right), \qquad [A.8]$$

with the asymptotes $x = 0$ and $dx/x = -dz$ (which is, of course, unphysical). All hyperbolae meet in the (unphysical) point

$$x = \frac{r_p}{r_p - 1}(>1), \quad \frac{dx}{x} = 0.$$

For a given loading x the relative (and absolute) error dx/x (dx) decreases with increasing particle density. The curves [A.8] give, for a given density error dz, the loadings which one may measure, if one wants to keep the relative loading error below prescribed values.

These curves express, qualitatively, the fact that the loading error dx/x is (in units of dz) of the same order of magnitude as $1/x$. The error curves lie above a limiting curve, of the equation $(dx/x)/dz = (1/x) - 1$, which would correspond to an infinite particle density $r_p = \infty$. The views on accuracy may be represented by the question: How precise has one to measure the density r_{tot}, in order to measure the loading x with an error dx/x smaller than a given quantity? Again this is the curves [A.8], but now looked upon with dx/x as parameter.

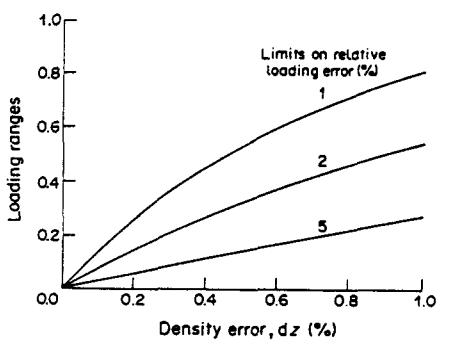

Figure A3. Loading ranges accessible with various errors of density measurements for prescribed limits on the loading errors.

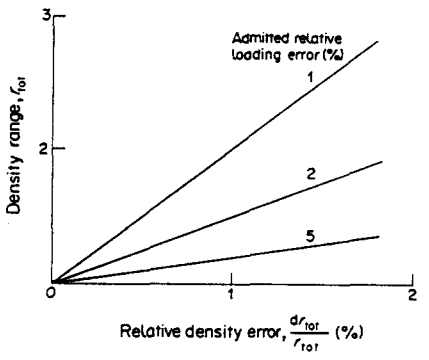

Figure A4. Accessibility range of the relative density r_{tot} for loading measurements, and its dependence on the relative density error dr_{tot}/r_{tot}, for various allowed limits on the relative loading error.

The inequality

$$x \geqslant \frac{r_p}{r_p - 1} \cdot \frac{dz}{\frac{dx}{x} + dz}, \qquad [A.9]$$

is illustrated in figure A3 for a sand–water mixture with the parameter dx/x taking the values 1, 2 and 5%.

A variant of this question is the following: What are the limitations in the (relative) density range r_{tot} as a function of the (relative) density errors dr_{tot}/r_{tot} for preassigned (relative) loading errors dx/x? The answer is contained in the (linear) inequality

$$r_{tot} \geqslant 1 + \frac{\left(\frac{dr_{tot}}{r_{tot}}\right)}{\left(\frac{dx}{x}\right)} \qquad [A.10]$$

(independent of the solid density) and is illustrated in figure A4.

The accuracy considerations made here from various points of view give an insight into the range where one expects density measurements of loadings to be reasonable precise. For loadings below 10% one has to have, in order to get errors of the order of 1–2%, a relative precision of the density determination of the order of 0.1%. Further, if one has

$$r_{tot} = \frac{\dot{m}_{tot}}{\dot{V}_{tot}} \cdot \frac{1}{\rho_f}$$

and, therefore,

$$\frac{dr_{tot}}{r_{tot}} = \frac{d\dot{m}_{tot}}{\dot{m}_{tot}} + \frac{d\dot{V}_{tot}}{\dot{V}_{tot}},$$

this would require relative errors $d\dot{m}_{tot}/\dot{m}_{tot}$, $d\dot{V}_{tot}/\dot{V}_{tot}$ of the order of 0.05%.

On the other hand, the considerations on loading are limited (from above) by the fact that the flow mechanism changes drastically. This happens for the water–sand mixture at a loading of about 30%, depending on the flow regime and velocity.